AJNR

Baseline Gadolinium Enhancement of the Intracranial Aneurysm Wall and Three-Dimensional Morphological Change During Long-Term Follow-Up

Maarten J. Kamphuis, Laura T. van der Kamp, Jari T. van Vliet, Ruben P.A. van Eijk, Jeroen Hendrikse, Gabriel J.E. Rinkel, Mervyn D.I. Vergouwen and Irene C. van der Schaaf

AJNR Am J Neuroradiol published online 7 May 2025
http://www.ajnr.org/content/early/2025/05/07/ajnr.A8825

ORIGINAL RESEARCH

Baseline Gadolinium Enhancement of the Intracranial Aneurysm Wall and Three-Dimensional Morphological Change During Long-Term Follow-Up

Maarten J. Kamphuis,* Laura T. van der Kamp,* Jari T. van Vliet, Ruben P.A. van Eijk, Jeroen Hendrikse, Gabriel J.E. Rinkel, Mervyn D.I. Vergouwen, Irene C. van der Schaaf
* These authors contributed equally.

ABSTRACT

BACKGROUND AND PURPOSE: Previous studies showed that intracranial aneurysm wall enhancement (AWE) is associated with aneurysm growth or rupture. These studies assessed growth with manual 2D measurements or eyeballing, both of which are prone to interobserver variability. To minimize this variability, we assessed the association between AWE and semi-automatically quantified 3D morphological changes in aneurysms during long-term follow-up.

MATERIALS AND METHODS: We included patients with an unruptured intracranial aneurysm who had baseline MR aneurysm wall imaging and were followed with MR or CT angiography for ≥1 year. We used in-house-developed software to measure six 3D morphological parameters on paired baseline and follow-up scans and determined changes over time. We compared the proportion of aneurysms showing morphological change (modified Z-score <-3.5 or >+3.5) between aneurysms with and without AWE. The risk difference with 95% CI was calculated for each morphological parameter. For parameters with a statistically significant change difference between aneurysms with and without AWE, we calculated ORs with 95% CI in a univariable logistic regression model, and adjusted for aneurysm size in a bivariable model.

RESULTS: Sixty-two patients with 72 unruptured intracranial aneurysms met inclusion criteria. Twenty aneurysms (28%) in 18 patients showed AWE at baseline. Median follow-up was 5.8 years (IQR 4.6–6.6). For the parameter curvedness, the proportion of aneurysms showing an increase was higher in aneurysms with AWE (6 of 20, 30%) than aneurysms without AWE (2 of 52, 4%), with a risk difference of 26% (95%CI 9–49%). For the other five morphological parameters, the proportion of aneurysms with morphological change was comparable between aneurysms with and without AWE. In logistic regression analysis, AWE was associated with curvedness increase (crude OR 10.7 [95%CI 2.2–78.9], adjusted OR 6.1 [95%CI 1.01–50.3]).

CONCLUSIONS: AWE was associated with aneurysm shape change during long-term follow-up, with an increase in 3D quantified curvedness that was independent of aneurysm size. This reinforces previous findings that AWE is associated with aneurysm instability, in particular curvedness increase, and suggests that curvedness could be a suitable parameter to capture aneurysm instability. Future studies need to investigate whether an increase in this parameter predicts aneurysmal rupture.

ABBREVIATIONS: AWE = aneurysm wall enhancement; AWI = aneurysm wall imaging; IBSI = imaging biomarker standardization initiative; UIA = unruptured intracranial aneurysm.

Received December 19, 2024; accepted after revision April 14, 2025.

From the Department of Radiology (M.J.K., J.T.v.V., J.H., I.C.v.d.S.), Department of Neurology and Neurosurgery, UMC Utrecht Brain Center (M.J.K., L.T.v.d.K., R.P.A.v.E., M.D.I.V., G.J.E.R.), and Biostatistics & Research Support, Julius Center for Health Sciences and Primary Care (R.P.A.v.E), University Medical Center Utrecht, Utrecht University, Utrecht, The Netherlands.

Mervyn D.I. Vergouwen is supported by a Clinical Established Investigator Grant by the Dutch Heart Foundation (2018T076) and has received funding from Bayer BV for investigator-initiated research unrelated to the current study (paid to institution). All other authors have nothing to disclose.

Please address correspondence to Maarten J. Kamphuis, MD, Department of Radiology, University Medical Center Utrecht, Utrecht, Heidelberglaan 100, Utrecht, 3584 CX, The Netherlands, m.j.kamphuis-5@umcutrecht.nl.

SUMMARY SECTION

PREVIOUS LITERATURE: Previous studies have shown that intracranial aneurysm wall enhancement (AWE) is associated with aneurysm instability. However, these studies relied on manual 2D size measurements or visual assessment, both of which are prone to interobserver variability. Change in 3D morphological parameters offers a more objective and potentially more suitable assessment of aneurysm instability. The relationship between AWE and 3D morphological changes over long-term follow-up has also not been well established. Our study aims to address this by evaluating the association between AWE and 3D quantified morphological changes over long-term follow-up.

KEY FINDINGS: AWE at baseline was associated with an increase in 3D quantified curvedness over long-term follow-up (median: 5.8 years). The proportion of aneurysms showing increased curvedness was significantly higher in those with AWE (30%) than in those without (4%), which was independent of aneurysm size (OR 6.1, 95% CI 1.01–50.3).

KNOWLEDGE ADVANCEMENT: This study provides evidence that AWE is associated with aneurysm shape change, especially an increase in curvedness, suggesting it as a potential marker of instability. Future research should explore whether an increase in curvedness predicts rupture.

Copyright 2025 by American Society of Neuroradiology.

INTRODUCTION

After an unruptured intracranial aneurysm (UIA) is diagnosed, the risk of rupture needs to be weighed against the risk of complications from endovascular or neurosurgical treatment to guide clinical management.[1] Current clinically used prediction models for aneurysm growth and rupture are based on patient and aneurysm characteristics,[2,3] but their discriminatory performance is limited, especially for aneurysms <7 mm in size.[4,5] To improve risk prediction for small aneurysms, additional predictors are needed. One potential predictor is aneurysm wall enhancement (AWE) with gadolinium-enhanced MR aneurysm wall imaging (MR-AWI). Previous longitudinal studies found that baseline AWE predicted instability (aneurysm growth, shape change, or rupture) during follow-up,[6–10] but a large cohort study showed that this was not independent of aneurysm size.[9] These studies used manual 2D measurements to determine aneurysm growth and eyeballing to assess morphological change, which are prone to interobserver variability. Three-dimensional quantified morphological parameters can minimize interobserver variability[11] and can therefore be used to detect associations between AWE and subtle morphological changes that would otherwise go undetected.[12] Moreover, previous studies had relatively short follow-up periods, with the longest having a median of 2.8 years.[10] Therefore, our aim was to investigate whether AWE at baseline is associated with 3D morphological change during long-term follow-up of intracranial aneurysms.

MATERIALS AND METHODS

Design and Population

The institutional review board of University Medical Center Utrecht, the Netherlands, waived formal ethical assessment and the requirement for informed consent because of the retrospective nature of the study (NedMec, 22-737). This study was performed at University Medical Center Utrecht, which serves as a tertiary referral center for patients with intracranial aneurysms. Patients were derived from the LUMINA (gadoLiniUM-enhanced aneurysm wall Imaging of Non-ruptured intracranial Aneurysms) study, which was performed in 2014–2015 to assess determinants of AWE at baseline.[13] All patients from that study were included in the current study if they had an unruptured intradural aneurysm for which follow-up imaging with TOF MRA or CTA had been performed for clinical reasons at least 1 year after initial MR-AWI. This study followed the Strengthening the Reporting of Observational Studies in Epidemiology (STROBE) reporting guidelines.

Patient and Aneurysm Characteristics

The following patient and aneurysm characteristics were collected as part of the previous study:[13] sex, age, history of subarachnoid hemorrhage from another aneurysm, hypertension (defined as either a diagnosis of hypertension or use of antihypertensive medication), and smoking status. Patients were categorized as current or former/never smokers. Patients were considered former smokers if they stopped smoking >3 months before baseline MR-AWI. Aneurysm size, location, and the presence of AWE on the baseline scan were recorded as part of the previous study[13] by an interventional neuroradiologist (I.C.v.d.S.) and a neuroradiologist (J.H.), each with >10 years of experience. Both radiologists were blinded to patient characteristics and outcome data were not available at the time of AWE assessment. AWE was assessed qualitatively: it was recorded as present if there was a definite hyperintensity in the aneurysm wall on MR-AWI after gadolinium administration that was not present on MR-AWI before gadolinium administration. This assessment method was shown to have excellent inter-observer reliability in previous studies.[10,14]

Baseline Aneurysm Wall Imaging

The MR-AWI protocol has been described previously.[13] Briefly, images were acquired in 2014–2015 using a 3T MRI scanner (Philips Healthcare, Best, the Netherlands), with an MR-AWI sequence acquired before and after administration of 0.1 mmol/kg gadobutrol (Gadovist 1.0 ®, Bayer AG, Leverkusen, Germany). In addition, a 3D TOF MRA sequence was acquired. See Online Supplemental Data for imaging parameters.

3D Morphological Measurements

If patients were followed up with multiple scans, we used the most recent follow-up scan for analysis. We performed manual 3D morphological measurements on baseline and follow-up TOF MRA or CTA images as described previously.[12] A contour was drawn around the aneurysm, and a mesh was fitted using in-house developed software implemented in MeVisLab (MeVis Medical Solutions). The major, minor, and least axis length (illustrated in Online Supplemental Data) were calculated with principal component analysis. The following morphological parameters were calculated according to the Imaging Biomarker Standardization Initiative (IBSI) guidelines:[15] volume, sphericity, elongation, and flatness. Sphericity is a ratio of volume to surface area; lower values correspond to a large surface area relative to volume. Elongation is a ratio of minor axis to major axis; lower values correspond to a more elongated shape. Flatness is a ratio of least axis to major axis; lower values correspond to a flatter shape. In addition, two local shape descriptors were determined based on the mesh: shape index and curvedness.[16] Shape index indicates whether the local shape is concave (low values) or convex (high values). Curvedness describes whether local curvatures are strong (high values) or weak (low values). These values were determined for every point on the mesh, and the median was calculated. Annotations were performed by M.J.K. (>3 years of experience) who was blinded to patient characteristics and the presence of AWE. These methods have been validated in a previous study, which showed good interobserver reliability for volumetric change.[11]

Assessment of Morphological Change

Changes over time in morphological parameters were calculated by subtracting the baseline scan values from the follow-up scan values. Morphological change was defined as a modified Z-score of change in morphological parameters exceeding a threshold of < -3.5 or > +3.5. The modified Z-score of the change in morphological parameter values between baseline and follow-up was determined for each aneurysm as: $\frac{0.675(x_i-\tilde{x})}{MAD}$, where x_i is the change in morphological parameter value between baseline and follow-up for each aneurysm, $\tilde{x}$ is the median change, and *MAD* is the median absolute deviation: $median\{|x_i - \tilde{x}|\}$.[12] It is a more robust method for detecting outliers than the standard Z-score, as it uses the median absolute deviation instead of the standard deviation.[17] The threshold of 3.5 allowed us to identify aneurysms whose morphology changed more than expected based on trends in the study population, and to study true morphological change rather than measurement variation.[17] The direction of change (increase or decrease) for which the 3.5 threshold value was taken, was based on a systematic review.[18] We tested for an increase in volume exceeding a modified Z-score of +3.5 and for a decrease in sphericity, elongation, and flatness below a modified Z-score of -3.5. Shape index and curvedness were not described in that systematic review, but low shape index values indicate surface concavities,[16] which are more common in aneurysms with irregular shapes.[12] Therefore, we tested for a decrease in shape index below a modified Z-score of -3.5. Higer values of curvedness indicate areas with stronger curvatures,[16] suggesting a more irregular shape.[12] Consequently, we tested for an increase in curvedness exceeding a modified Z-score of +3.5.

Statistical Analysis

We compared baseline patient and aneurysm characteristics between aneurysms with and without AWE with a two-sided Fisher exact or Chi square test for categorical variables, and a student's t-test or Mann-Whitney U test for continuous variables, as appropriate. We assessed the association between AWE and morphological change for each of the six morphological parameter separately. The absolute risk difference for change in each morphological parameter between aneurysms with and without AWE was calculated, along with the 95% CI according to Miettinen and Nurminen.[19] As a sensitivity analysis, we performed a patient-based analysis, selecting the largest UIA in the case of multiple UIAs per patient, in line with previous studies.[2,3] The parameters with a statistically significant change difference between aneurysms with and without AWE were analyzed using univariable logistic regression. The change in morphological parameter (based on the modified Z-score threshold of 3.5) was used as the dependent variable and AWE as the independent variable. In a bivariable model, we adjusted for aneurysm size, as this was a confounder in a previous study.[9] Results were reported as OR with 95% CI. R version 4.2.1 with the DescTools package was used for analyses.

RESULTS

Seventy-six patients with 87 aneurysms underwent baseline MR-AWI, of whom 62 patients with 72 aneurysms were followed with imaging for at least 1 year. One patient was excluded because of rupture during follow-up without imaging before rupture (this aneurysm showed AWE). The majority of patients (48/62, 77%) was female, and the mean age at baseline was 57 years (standard deviation 9 years). Aneurysms with AWE were larger (p-value <.001) and had a different location distribution (p-value <.002), being more often located in the middle cerebral artery compared to aneurysms without AWE (Table 1). Ten patients had two aneurysms, and 5 of them had at least one aneurysm with AWE. Follow-up imaging was performed with TOF MRA in 53 patients (86%), and with CTA in 9 patients (15%). The total follow-up duration was 379 aneurysm-years (median follow-up 5.8 years, interquartile range 4.6–6.6 years). Twenty of 72 aneurysms (28%) showed AWE at baseline.

Table 1: Baseline patient and aneurysm characteristics.

		Aneurysm wall enhancement at baseline		
Patient characteristics[a]	All (n=62)	Present (n=18)	Absent (n=44)	p-value
Female sex	48 (77)	13 (72)	35 (80)	.77[d]
Mean age (SD)	57 (9)	59 (8)	56 (10)	.16[e]
History of SAH	13 (21)	4 (22)	9 (21)	1.00[f]
Hypertension	32 (52)	10 (56)	22 (50)	.91[d]
Current smoker[b]	17 (27)	5 (28)	12 (27)	1.00[d]
Multiple aneurysms	10 (16)	5 (28)	5 (11)	.22[d]
Aneurysm characteristics	All (n=72)	Present (n=20)	Absent (n=52)	p-value
Median size, mm (IQR)	4.4 (2.7–6.0)	6.1 (5.1–8.4)	3.8 (2.5–5.3)	**<.001**[g]
Location				**.002**[f]
ACA/ACom	12 (17)	1 (5)	11 (21)	
ICA/PCom	22 (31)	2 (10)	20 (39)	
MCA	32 (44)	16 (80)	16 (31)	
Posterior circulation	6 (8)	1 (5)	5 (10)	
Median follow-up, years (IQR)	5.8 (4.6–6.6)	5.5 (2.1–6.6)	6.0 (5.0–6.7)	.27[g]
Median 3D morphological parameter values (IQR)	All (n=72)	Present (n=20)	Absent (n=52)	
Volume (mm^3)	41 (12–83)	73 (53–141)	25 (11–58)	

Sphericity[c]	82 (79–84)	81 (78–84)	82 (80–84)
Elongation[c]	87 (82–91)	87 (84–90)	87 (81–91)
Flatness[c]	78 (73–83)	82 (76–83)	77 (72–83)
Shape index[c]	50 (33–50)	33 (26–43)	50 (41–50)
Curvedness	2.3 (2.3–2.4)	2.3 (2.3–2.4)	2.3 (2.3–2.5)

Values are displayed as n (%) unless indicated otherwise. p-values reflect the comparison between aneurysms with and without aneurysm wall enhancement. SD, standard deviation; IQR, interquartile range; ACA, anterior cerebral artery; ACom, anterior communicating artery; ICA, internal carotid artery; PCom, posterior communicating artery; MCA, middle cerebral artery.
Bold typeface indicates statistical significance.
[a] Patients were stratified for wall enhancement according to the largest aneurysm.
[b] Patients were classified as current smokers if they had smoked within three months prior to MR-AWI.
[c] Values were multiplied by 100.
[d] Chi square test.
[e] Unpaired t-test.
[f] Fisher exact test.
[g] Mann Whitney U test.

An increase in curvedness was found in 6 of 20 aneurysms with AWE (30%) and in 2 of 52 aneurysms without AWE (4%), with an absolute risk difference of 26% (95% CI 9 to 49%) (Table 2; Online Supplemental Data). An increase in volume was found in 3 of 20 aneurysms with AWE (15%) and in 2 of 52 aneurysms without AWE (4%), with an absolute risk difference of 11% (95% CI -2 to 33). For the other four morphological parameters, sphericity, elongation, flatness, and shape index, the proportion of aneurysms with change was comparable between aneurysms with and without AWE. The patient-based sensitivity analysis yielded similar results: an increase in curvedness was found in 5 of 18 aneurysms with AWE (28%) and 2 of 44 aneurysms without AWE (5%), with an absolute risk difference of 23% (95% CI 5 to 47%) (Online Supplemental Data).

Table 2: Change in morphological parameters during follow-up stratified for aneurysm wall enhancement.

Parameter	Modified Z-score threshold for morphological change[a]	Total (n=72)	Wall enhancement (n=20)	No wall enhancement (n=52)	Absolute risk difference (95% CI)[b]
Volume	> 3.5	5 (7%)	3 (15%)	2 (4%)	11% (-2 to 33%)
Sphericity	< -3.5	0 (0%)	0 (0%)	0 (0%)	0% (-7 to 16%)
Elongation	< -3.5	2 (3%)	0 (0%)	2 (4%)	-4% (-13 to 13%)
Flatness	< -3.5	1 (1%)	0 (0%)	1 (2%)	-2% (-10 to 14%)
Shape index	< -3.5	17 (24%)	5 (25%)	12 (23%)	2% (-18 to 26%)
Curvedness	> 3.5	8 (11%)	6 (30%)	2 (4%)	**26% (9 to 49%)**

Bold typeface indicates statistical significance.
[a] Morphological change was defined as a modified Z-score >3.5 or < -3.5, depending on the known direction of change that corresponds with aneurysm instability.
[b] Absolute risk difference of aneurysm instability in aneurysms with wall enhancement compared to aneurysms without wall enhancement; 95% CI calculated according to Miettinen and Nurminen.

In univariable logistic regression analysis, AWE was associated with curvedness increase (OR 10.7, 95% CI 2.2–78.9). The bivariable model showed that this was independent of aneurysm size (OR 6.1, 95% CI 1.01–50.3). An example case of an aneurysm with AWE and an increase in curvedness and volume is shown in Figure 1.

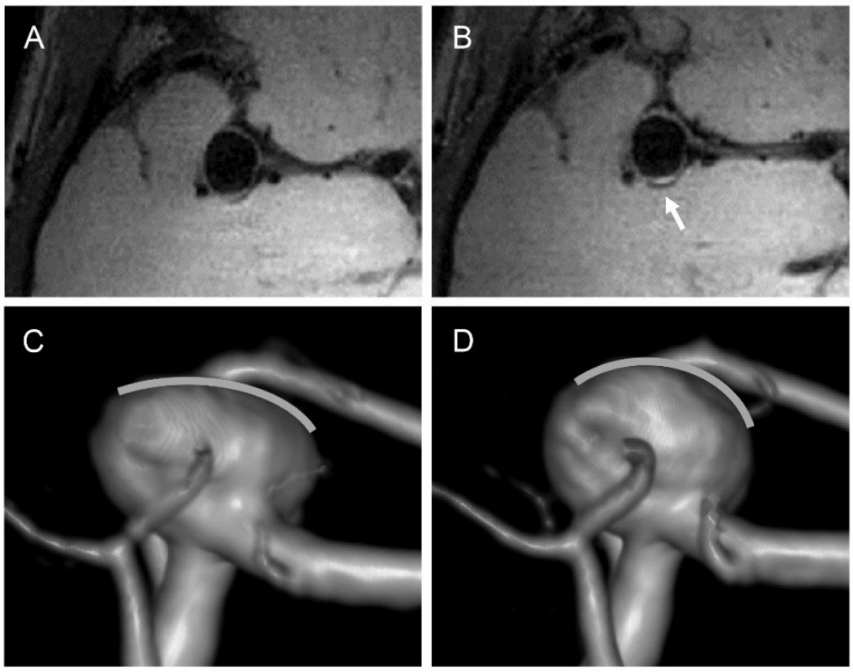

FIG 1. Example of aneurysm with wall enhancement at baseline and increase in curvedness during follow-up. Figures show a 9-mm aneurysm at the right middle cerebral artery bifurcation. *A*, Axial view of the aneurysm on MR aneurysm wall imaging at baseline before gadolinium administration. *B*, After gadolinium administration, aneurysm wall enhancement is seen on the dorsal side of the aneurysm (arrow). *C*, Multiplanar reconstruction of time-of-flight MR angiography at baseline and, *D*, at follow-up 1 year later. Lines in C and D indicate a location of increased curvedness over time. The aneurysm increased in volume by 193 mm3 (from 412 to 605 mm3), corresponding to a modified Z-score of 24. Its median curvedness increased by 0.5 (from 1.8 to 2.3), corresponding to a modified Z-score of 4.5. Modified Z-scores exceeding 3.5 were considered to reflect true changes rather than measurement variation.

DISCUSSION

AWE was associated with an increase in 3D quantified curvedness on long-term follow-up, independent of aneurysm size. For the other morphological parameters, no difference in change was found between aneurysms with and without AWE, although there was a trend towards more frequent volume increases in aneurysms with AWE compared to those without AWE.

A previous international cohort study of 455 patients with 559 aneurysms showed that AWE was a predictor of aneurysm growth, defined as ≥1 mm size increase in 2D measurements, or rupture during a median follow-up period of 1.2 years, but not independent of aneurysm size.[9] A second study of 129 patients with 145 aneurysms also found that AWE was a predictor of aneurysm instability (≥1 mm size increase or appearance of an irregular shape) during a median follow-up duration of 2 years.[7] Three other studies similarly showed that the presence of AWE was associated with aneurysm instability during median follow-up periods of 1.3–2.8 years.[6,8,10] All previous studies defined aneurysm instability as manually measured 2D growth or as visually assessed morphological change. In contrast, we used 3D quantified morphological change, which is more reliable[11] and allowed for the detection of subtle morphological change that would probably have remained undetected with visual assessment.[12] In addition, our study had a longer median follow up of 5.8 years compared to previous studies.

Since previous studies have reported associations between AWE and 2D growth,[6–10] we expected to find an association between AWE and volumetric increase. However, we only found a trend for an association between AWE and volumetric increase, whereas we found a statistically significant association between AWE and curvedness increase. An increase in curvedness is related to protrusion of the vessel wall.[12] It is possible that curvedness increase is an early indicator of aneurysm instability and may therefore serve as an early marker for detecting aneurysm changes, potentially even more sensitive than volume. A previous study found an association between aneurysm growth and a *decrease* in curvedness.[12] However, that study examined the relationship between change in volume and change in curvedness, whereas we investigated the relationship between aneurysm wall enhancement and change in curvedness. This does not represent a true discrepancy, as the studies focused on different associations.

A strength of our study is that we used a longitudinal design with a much longer median follow-up period than previous studies.[10] Another strength is that AWE assessment was performed before outcome data were available and that morphological measurements were performed blinded for the presence of AWE.[11]

There are some limitations. First, the number of aneurysms showing morphological change was relatively small for most parameters, which allowed us to adjust for only one confounder. Part of the association between AWE and curvedness increase may also be confounded by aneurysm location and future studies in larger cohorts should also include aneurysm location in multivariable analysis. Second, we had to exclude one patient with an aneurysm that ruptured during follow-up, because no follow-up imaging was available before rupture and post-rupture morphology would not be representative of pre-rupture morphology.[20,21] Third, follow-up imaging protocols were not

standardized. Most aneurysms were followed with TOF MRA and some with CTA, depending on the physician's and patient's preference. However, previous research has demonstrated that intracranial aneurysm 3D morphological parameters are highly comparable across imaging modalities. A recent study of 55 patients with 65 aneurysms demonstrated that most 3D morphological parameters show good to excellent reliability across MRA, CTA, and DSA.[22] In addition, two studies of 21 and 10 patients, respectively, found no significant differences in aneurysm geometry between modalities.[23,24] We resampled images to identical voxel size to further mitigate potential modality-dependent differences. Finally, the etiology of AWE is incompletely understood. While it has been linked to inflammation,[25] some AWE signal may also result from incomplete suppression of non-laminar and slow-flowing blood near the aneurysm wall.[26]

COCLUSIONS

We found that AWE is associated with aneurysm shape change during long-term follow-up, in particular an increase in curvedness, and that this was independent of aneurysm size. Curvedness may be a suitable parameter for assessing aneurysm instability, although future studies should investigate whether an increase in curvedness is also associated with aneurysmal rupture. In addition, research should be conducted in larger cohorts to confirm our findings, which would be feasible with the availability of automated aneurysm segmentation tools.[27]

ACKNOWLEDGMENTS

The authors used ChatGPT-4o in order to enhance the flow and grammatical accuracy of the manuscript. The authors reviewed and edited the content as needed and take full responsibility for the text's factual accuracy and originality.

REFERENCES

1. Etminan N, de Sousa DA, Tiseo C, et al. European Stroke Organisation (ESO) guidelines on management of unruptured intracranial aneurysms. Eur Stroke J 2022;7:LXXXI–CVI. DOI: 10.1177/23969873221099736
2. Greving JP, Wermer MJH, Brown RD, et al. Development of the PHASES score for prediction of risk of rupture of intracranial aneurysms: a pooled analysis of six prospective cohort studies. Lancet Neurol 2014;13:59-66. DOI: 10.1016/S1474-4422(13)70263-1
3. Backes D, Rinkel GJE, Greving JP, et al. ELAPSS score for prediction of risk of growth of unruptured intracranial aneurysms. Neurology 2017;88:1600-1606. DOI: 10.1212/WNL.0000000000003865
4. Rutledge C, Jonzzon S, Winkler EA, Raper D, Lawton MT, Abla AA. Small aneurysms with low PHASES scores account for most subarachnoid hemorrhage cases. World Neurosurg 2020;139:e580-e584. DOI: 10.1016/j.wneu.2020.04.074
5. Pettersson SD, Skrzypkowska P, Pietrzak K, et al. Evaluation of PHASES score for predicting rupture of intracranial aneurysms: significance of aneurysm size. World Neurosurg 2024;184:e178-e184. DOI: 10.1016/j.wneu.2024.01.077
6. Vergouwen MDI, Backes D, Van Der Schaaf IC, et al. Gadolinium enhancement of the aneurysm wall in unruptured intracranial aneurysms is associated with an increased risk of aneurysm instability: a follow-up study. AJNR Am J Neuroradiol 2019;40:1112-1116. DOI: 10.3174/ajnr.A6105
7. Gariel F, Ben Hassen W, Boulouis G, et al. Increased wall enhancement during follow-up as a predictor of subsequent aneurysmal growth. Stroke 2020;51:1868-1872. DOI: 10.1161/STROKEAHA.119.028431
8. Yang CY, Wen L, Cui C, et al. A prospective follow-up study on risk factors to predict the progression of unruptured intracranial aneurysms on enhanced HR-MRI. Acad Radiol 2022;30:1247-1256. DOI: 10.1016/j.acra.2022.10.014
9. Van der Kamp LT, Edjlali M, Naggara O, et al. Gadolinium-enhanced intracranial aneurysm wall imaging and risk of aneurysm growth and rupture: a multicentre longitudinal cohort study. Eur Radiol 2023;34:4610-4618. DOI: 10.1007/s00330-023-10388-7
10. Hashimoto Y, Matsushige T, Kawano R, et al. Focal aneurysm wall enhancement in vessel wall imaging as a surrogate marker for predicting aneurysm instability. Stroke Vasc Interv Neurol 2023;3:e001029. DOI: 10.1161/SVIN.123.001029
11. Timmins KM, Kuijf HJ, Vergouwen MDI, et al. Reliability and agreement of 2D and 3D measurements on MRAs for growth assessment of unruptured intracranial aneurysms. AJNR Am J Neuroradiol 2021;42:1598-1603. DOI: 10.3174/ajnr.A7186
12. Timmins KM, Kuijf HJ, Vergouwen MDI, Ruigrok YM, Velthuis BK, van der Schaaf IC. Relationship between 3D morphologic change and 2D and 3D growth of unruptured intracranial aneurysms. AJNR Am J Neuroradiol 2022;43:416-421. DOI: 10.3174/ajnr.A7418
13. Backes D, Hendrikse J, van der Schaaf I, et al. Determinants of gadolinium-enhancement of the aneurysm wall in unruptured intracranial aneurysms. Neurosurgery 2018;83:719-725. DOI: 10.1093/neuros/nyx487
14. Matsushige T, Shimonaga K, Ishii D, et al. Vessel wall imaging of evolving unruptured intracranial aneurysms. Stroke 2019;50:1891-1894. DOI: 10.1161/STROKEAHA.119.025245

15. Zwanenburg A, Vallières M, Abdalah MA, et al. The image biomarker standardization initiative: standardized quantitative radiomics for high-throughput image-based phenotyping. Radiology 2020;295:328-338. DOI: 10.1148/radiol.2020191145

16. Koenderink J, Doorn A. Surface shape and curvature scales. Image Vis Comput 1992;10:557-564. DOI: 10.1016/0262-8856(92)90076-F

17. Iglewicz B, Hoaglin DC. How to detect and handle outliers. In: Mykytka EF, ed. The ASQC Basic References in Quality Control: Statistical Techniques. Vol 16. Milwaukee: ASQ Quality Press; 1993:11-13

18. Johnson MD, Palmisciano P, Yamani AS, Hoz SS, Prestigiacomo CJ. A systematic review and meta-analysis of 3-dimensional morphometric parameters for cerebral aneurysms. World Neurosurg 2024;183:214-226. DOI: 10.1016/j.wneu.2023.12.131

19. Miettinen O, Nurminen M. Comparative analysis of two rates. Stat Med 1985;4:213-226. DOI: 10.1002/sim.4780040211

20. Skodvin TO, Johnsen LH, Gjertsen Ø, Isaksen JG, Sorteberg A. Cerebral aneurysm morphology before and after rupture: nationwide case series of 29 aneurysms. Stroke 2017;48:880-886. DOI: 10.1161/STROKEAHA.116.015288

21. Kamphuis MJ, Timmins KM, Kuijf HJ, et al. Three-dimensional morphological change of intracranial aneurysms before and around rupture. Neurosurgery 2024;94:1211-1217. DOI: 10.1227/neu.0000000000002812

22. Johnson MD, Street S, Prestigiacomo CJ. Inter-modality correlation across invasive and noninvasive angiography in the three-dimensional assessment of cerebral aneurysms. Surg Neurol Int 2025;16:1-8. DOI: 10.25259/SNI_1019_2024

23. Wang X, Benson JC, Jagadeesan B, McKinney A. Giant cerebral aneurysms: comparing CTA, MRA, and digital subtraction angiography assessments. J Neuroimaging 2020;30:335-341. DOI: 10.1111/jon.12712

24. Ren Y, Chen GZ, Liu Z, Cai Y, Lu GM, Li ZY. Reproducibility of image-based computational models of intracranial aneurysm: a comparison between 3D rotational angiography, CT angiography and MR angiography. Biomed Eng Online 2016;15:1-14. DOI: 10.1186/s12938-016-0163-4

25. Zhong W, Su W, Li T, et al. Aneurysm wall enhancement in unruptured intracranial aneurysms: a histopathological evaluation. J Am Heart Assoc 2021;10:1-10. DOI: 10.1161/JAHA.120.018633

26. Cornelissen BMW, Leemans EL, Coolen BF, et al. Insufficient slow-flow suppression mimicking aneurysm wall enhancement in magnetic resonance vessel wall imaging: a phantom study. Neurosurg Focus 2019;47. DOI: 10.3171/2019.4.FOCUS19235

27. Timmins KM, Van Der Schaaf IC, Vos IN, Ruigrok YM, Velthuis BK, Kuijf HJ. Geometric deep learning using vascular surface meshes for modality-independent unruptured intracranial aneurysm detection. IEEE Trans Med Imaging 2023;42:3451-3460. DOI: 10.1109/TMI.2023.3288746

Supplemental Figure. Histograms of change in 3D morphological parameters of intracranial aneurysms scaled with modified Z-score.

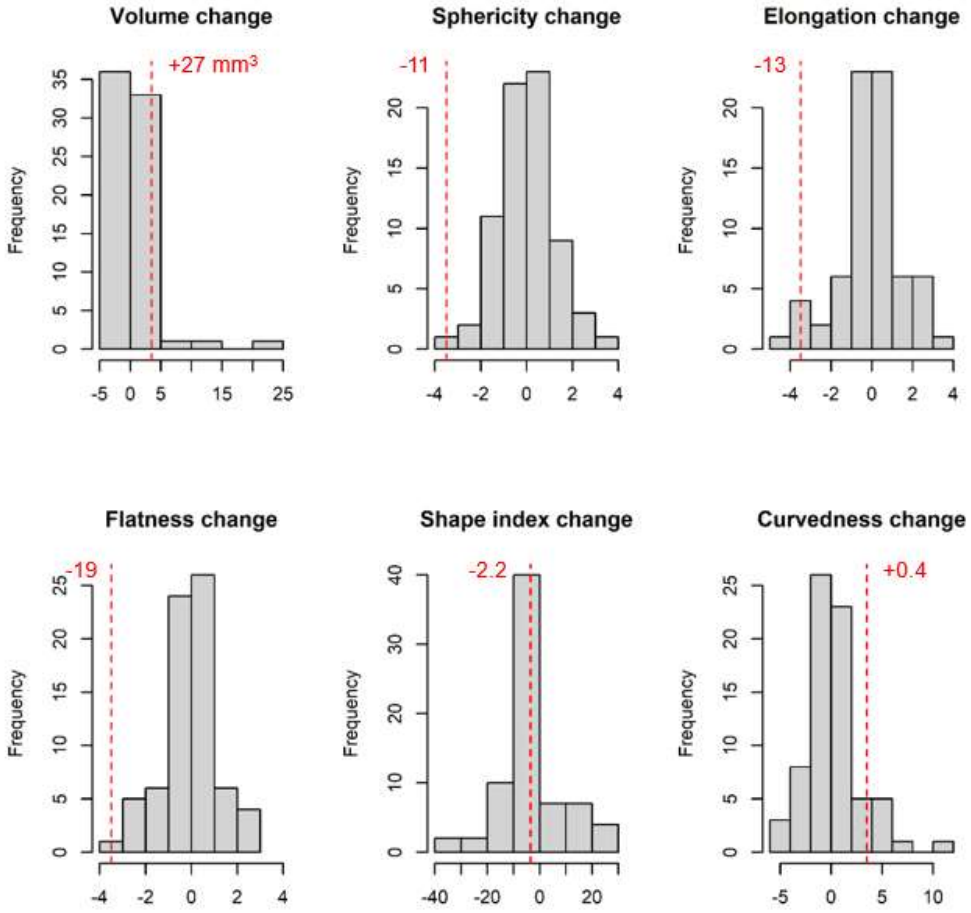

Red dashed lines indicate modified Z-scores of -3.5 or 3.5. A modified Z-score increase of > +3.5 was used to identify instable aneurysms for volume and curvedness, and a decrease of < -3.5 was used to identify instable aneurysms for the parameters sphericity, elongation, flatness, and shape index. Numbers in red indicate the absolute change in parameter values that correspond to the modified Z-scores of -3.5 or 3.5. These were multiplied by 100 for sphericity, elongation, flatness, and shape index, in line with Table 1. For example, aneurysms with volumetric increases of more than 27 mm^3 were considered to show true morphological change.

Supplemental Table. Change in morphological parameters during follow-up stratified for aneurysm wall enhancement at patient level.

Parameter	Modified Z-score threshold for morphological change[a]	Total (n=62)	Wall enhancement (n=18)	No wall enhancement (n=44)	Absolute risk difference (95% CI)[b]
Volume	> 3.5	4 (7%)	2 (11%)	2 (5%)	7% (-7 to 29%)
Sphericity	< -3.5	0 (0%)	0 (0%)	0 (0%)	0% (-8 to 18%)
Elongation	< -3.5	2 (3%)	0 (0%)	2 (5%)	-5% (-15 to 14%)
Flatness	< -3.5	1 (2%)	0 (0%)	1 (2%)	-2% (-12 to 16%)
Shape index	< -3.5	16 (26%)	4 (22%)	12 (27%)	-5% (-26 to 21%)
Curvedness	> 3.5	7 (11%)	5 (28%)	2 (5%)	**23% (5 to 47%)**

In case of multiple aneurysms per patient, the largest aneurysm was selected. Bold typeface indicates statistical significance.
[a] Morphological change was defined as a modified Z-score of < -3.5 or > +3.5, depending on the known direction of change that

corresponds with aneurysm instability.
[b] Absolute risk difference of aneurysm instability in aneurysms with wall enhancement compared to aneurysms without wall enhancement; 95% CI calculated according to Miettinen and Nurminen.

Supplemental Table. Morphological parameters according to the Imaging Biomarker Standardization Initiative.

Parameter	Mathematical definition	Low	High
Volume[a]	$\left\lvert \sum_{k=1}^{N_{fc}} V_k \right\rvert$		
Elongation[b]	$\sqrt{\frac{\lambda_{minor}}{\lambda_{major}}}$	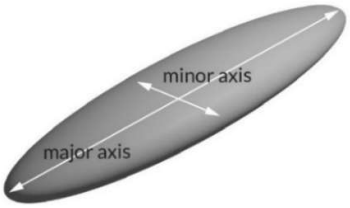	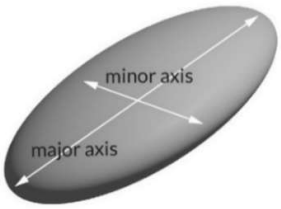
Flatness[b]	$\sqrt{\frac{\lambda_{least}}{\lambda_{major}}}$	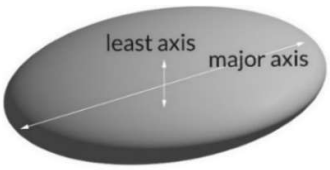	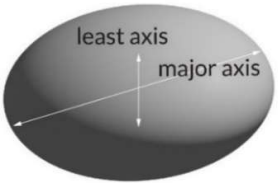
Sphericity[c]	$\frac{\left(36\pi V^2\right)^{1/3}}{A}$		

[a] Volume is calculated by summing the signed volumes of each tetrahedron in the mesh: $V_k = \frac{a \cdot (b \times c)}{6}$, where a, b, and c represent the vertex points of face k.
[b] Parameters are based on λ_{major}, λ_{minor}, and λ_{least}, which correspond to the major, minor, and least axis of the triaxial ellipsoid, respectively.
[c] Parameter is based on volume (V) and surface area (A). Shapes with high surface area relative to volume have lower values.

Supplemental Table. TOF MRA scan parameters (Philips Achieva 3 Tesla).

Parameter	Value
SmartSelect	Yes
Coil 1 (exclude)	None
Uniformity	CLEAR
FOV (mm)	
AP	200
RL	200
FH	80
ACQ voxel size (mm)	
AP	0.403
RL	0.704
FH	1
Recon voxel size (mm)	
AP	0.357
RL	0.357
FH	0.5
Fold-over suppression	No
ENCASE enable	No
Reconstruction matrix	560
SENSE	Yes
P reduction (RL)	2.5
S reduction (FH)	1
CS-SENSE	No
k-t Acceleration	No
Stacks	1
Slices	160
Slice orientation	Transverse
Fold-over direction	RL
Fat shift direction	P
Multi-chunk	Yes
Chunks	4
Chunk scan order	HF
Large table movement	No
PlanAlign	No
REST slabs	1
Type	Parallel
Thickness (mm)	20
Position	Head
Gap	User-defined
(mm)	10

Power	1
Interactive positioning	No
Patient position	Head first
Patient body position	Head first
Patient orientation	Supine
Patient body orientation	Supine
Scan type	Imaging
Scan mode	3D
Technique	FFE
3D non-selective	No
Loop order	zy_order
Contrast enhancement	T1
Acquisition mode	Cartesian
Fast Imaging mode	None
Echoes	1
Partial echo	Yes
Shifted echo	No
TE (ms)	3.45283341
Flip angle (deg)	18
TR (ms)	22
Halfscan	No
Water-fat shift (pixels)	2
RF Shims	Fixed
Shim	Default
mDIXON	No
Fat suppression	No
Water suppression	No
MTC	No
Custom prepulse	No
MDME	No
Diffusion mode	No
T1 mapping	No
Multi-transmit	Yes
Transmit channels	Both
SAR mode	High
B1 mode	User-defined
Amplitude (uT)	10.5
SAR allow first level	Yes
Patient pregnancy	No
Patient WB SAR [W/kg]	0
Patient Head SAR [W/kg]	0

Patient max. dB/dt [T/s]	0
Max slewrate [T/m/s]	0
Max. B1+rms [uT]	0
PNS mode	Moderate
Gradient mode	Maximum
SofTone mode	No
Cardiac synchronization	No
Heart rate > 250 bpm	No
Respiratory compensation	No
Navigator respiratory comp	No
Flow compensation	Yes
fMRI echo stabilisation	No
NSA	1
MRE enable	No
Angio / Contrast enh.	Inflow
Quantitative flow	No
Tone pulse	Yes
Start angle	16
Direction	F->H
Manual start	No
Dynamic study	No
Arterial Spin labeling	No
Preparation phases	Auto
Interactive F0	No
Quick Survey	Default
B0 field map	No
B1 field map	No
MIP/MPR	MIP
Protocol	Compose
SWIp	No
Images	M, (3) No
Autoview image	M
Calculated images	(4) No
Reference tissue	Blood
Recon compression	No
Preset window contrast	Soft
Reconstruction mode	Real-time
Save raw data	No
Hardcopy protocol	No
Image filter	System default
Uniformity correction	No

Geometry correction	Default
Elliptical k-space shutter	Default
Stack Offc. AP (P=+mm)	12.2004375
Stack Offc. RL (L=+mm)	8.15987587e-05
Stack Offc. FH (H=+mm)	43.7575226
Ang. AP (deg)	0
Ang. RL (deg)	0.0592882931
Ang. FH (deg)	-0
Free rotatable	No
Total scan duration	04:59.4
Rel. SNR	1
Act. TR/TE (ms)	22 / 3.5
ACQ matrix M x P	496 x 284
ACQ voxel MPS (mm)	0.40 / 0.70 / 1.00
REC voxel MPS (mm)	0.36 / 0.36 / 0.50
Scan percentage (%)	57.2864304
Chunk thickness (mm)	20
Packages	4
Act. slice gap (mm)	-0.5
Act. WFS (pix) / BW (Hz)	2.000 / 217.3
Min. WFS (pix) / Max. BW (Hz)	0.827 / 525.0
Min. TR/TE (ms)	15 / 2.2
Local torso SAR	< 70 %
Whole body SAR / level	< 1.8 W/kg / normal
SED	< 0.6 kJ/kg
Coil Power	67 %
Max B1+rms	1.91 uT
PNS / level	79 % / normal
dB/dt	81.9 T/s
Sound Pressure Level (dB)	17.943985

Supplemental Table. MR aneurysm wall imaging scan parameters (Philips Achieva 3 Tesla).

Parameter	Value
SmartSelect	yes
Coil 1 (exclude)	None
Uniformity	CLEAR
FOV (mm)	
AP	200
RL	166
FH	45
ACQ voxel size (mm)	
AP	0.5
RL	0.5
FH	1
Recon voxel size (mm)	
AP	0.5
RL	0.5
FH	0.5
Fold-over suppression	no
Slice oversampling	user defined
Oversample factor	1.79999995
Reconstruction matrix	400
SENSE	yes
P reduction (RL)	1.5
S reduction (FH)	1
CS-SENSE	no
k-t Acceleration	no
Stacks	1
Slices	90
Slice orientation	transverse
Fold-over direction	RL
Fat shift direction	P
Multi-chunk	no
O-MAR	no
Large table movement	no
PlanAlign	no
REST slabs	0
Interactive positioning	no
Patient position	head first
Patient body position	head first
Patient orientation	supine
Patient body orientation	supine

Scan type	Imaging
Scan mode	3D
Technique	SE
Modified SE	no
Acquisition mode	cartesian
Fast Imaging mode	TSE
3D VIEW	no
Shot mode	multishot
TSE factor	56
3D free factor	yes
Startup echoes	4
Profile order	low_high
Turbo direction	Y
DRIVE	anti
Ultrashort	ultra
FID reduction	default
3D non-selective	yes
Echoes	1
Partial echo	no
TE	shortest
Flip angle (deg)	90
Refocusing control	tissue specific
Signal plateau	min. angle defined
Min. angle (deg)	25
Max1 angle (deg)	120
Max2 angle (deg)	120
TR	user defined
TR (ms)	1500
Halfscan	no
Water-fat shift	minimum
RF Shims	adaptive
Shim	default
mDIXON	no
Fat suppression	no
Grad Rev Fat suppr	no
Water suppression	no
BB pulse	no
MTC	no
APT	no
Custom prepulse	no
MDME	no

Diffusion mode	no
T1 mapping	no
Multi-transmit	yes
Transmit channels	both
SAR mode	high
B1 mode	default
SAR allow first level	yes
Patient pregnancy	no
Patient WB SAR [W/kg]	0
Patient Head SAR [W/kg]	0
Patient max. dB/dt [T/s]	0
Max slewrate [T/m/s]	0
Max. B1+rms [uT]	0
PNS mode	moderate
Gradient mode	maximum
SofTone mode	no
Cardiac synchronization	no
Heart rate > 250 bpm	no
Respiratory compensation	no
Navigator respiratory comp	no
Flow compensation	no
Motion smoothing	no
NSA	1
MRE enable	no
CENTRA	no
Manual start	no
Dynamic study	no
Arterial Spin labeling	no
Preparation phases	auto
Interactive F0	no
Quick Survey	default
B0 field map	no
B1 field map	no
MIP/MPR	no
Images	M, (3) no
Autoview image	M
Calculated images	(4) no
Reference tissue	Grey matter
Recon compression	No
Preset window contrast	soft
Reconstruction mode	immediate

Save raw data	no
Hardcopy protocol	no
Image filter	system default
Uniformity correction	no
Geometry correction	none
Elliptical k-space shutter	no
Stack Offc. AP (P=+mm)	-28.6281986
Stack Offc. RL (L=+mm)	-3.86688972
Stack Offc. FH (H=+mm)	-3.385221
Ang. AP (deg)	3.7169652
Ang. RL (deg)	-16.0221748
Ang. FH (deg)	1.06650794
Free rotatable	no
IF_info_seperator	1634755923
Extended Function. Opt.	6
Total scan duration	08:03.0
Rel. SNR	1
Act. TR (ms)	1500
Act. TE (ms)	32
ACQ matrix M x P	400 x 332
ACQ voxel MPS (mm)	0.50 / 0.50 / 1.00
REC voxel MPS (mm)	0.50 / 0.50 / 0.50
Scan percentage (%)	100
Act. slice gap (mm)	-0.5
WFS (pix) / BW (Hz)	0.681 / 637.8
TSE es / shot (ms)	4.5 / 286
Plateau / TEeff / TEequiv	264 / 32 / 25
Min. TR (ms)	306
Local torso SAR	< 20 %
Whole body SAR / level	< 0.5 W/kg / normal
SED	< 0.3 kJ/kg
Coil Power	19 %
Max B1+rms	1.03 uT
PNS / level	79 % / normal
dB/dt	74.0 T/s
Sound Pressure Level (dB)	18.5135689